

Simulations of neutral beam injection and ion cyclotron resonance heating synergy in high power EAST scenarios

Cite as: Rev. Sci. Instrum. 93, 113501 (2022); doi: 10.1063/5.0101645

Submitted: 2 June 2022 • Accepted: 28 September 2022 •

Published Online: 1 November 2022



View Online



Export Citation



CrossMark

D. K. Yang,¹ L. Y. Liao,¹ Y. H. Li,¹ G. Q. Zhong,² X. J. Zhang,² W. Zhang,² B. L. Hao,² L. Q. Hu,² B. N. Wan,² Z. M. Hu,³ Y. M. Zhang,⁴ G. Gorini,^{5,6} M. Nocente,^{5,6} M. Tardocchi,⁶ X. Q. Li,¹ C. J. Xiao,^{1,a)} and T. S. Fan^{1,a)}

AFFILIATIONS

¹State Key Laboratory of Nuclear Physics and Technology, Peking University, Beijing 100871, China

²Institute of Plasma Physics, Chinese Academy of Sciences, Hefei 230031, Anhui, China

³Interdisciplinary InnoCentre for Nuclear Technology, Nanjing University, Nanjing 211106, Jiangsu, China

⁴China Academy of Engineering Physics, Mianyang 621900, Sichuan, China

⁵Dipartimento di Fisica "G. Occhialini," Università degli Studi di Milano-Bicocca, Milano 20126, Italy

⁶Institute for Plasma Science and Technology, National Research Council, Milan 20125, Italy

Note: This paper is part of the Special Topic on Proceedings of the 24th Topical Conference on High-Temperature Plasma Diagnostics.

^{a)}Authors to whom correspondence should be addressed: cjxiao@pku.edu.cn and tsfan@pku.edu.cn

ABSTRACT

The EAST plasmas heated with deuterium neutral beam injection and ion cyclotron resonance heating (ICRH) have been simulated by the TRANSP code. The analysis has been conducted using the full wave solver TORIC5, the radio frequency (RF)-kick operator, and NUBEAM to model the RF heating effects on fast ion velocity distribution. In this work, we present several simulated results compared with experiments for high power EAST scenarios, indicating that the interactions between ICRH and fast ions can significantly accelerate fast ions, which are confirmed by the increased neutron yield and broadened neutron emission spectrum measurements.

Published under an exclusive license by AIP Publishing. <https://doi.org/10.1063/5.0101645>

I. INTRODUCTION

In sustained fusion plasmas, heating is predominantly produced by the slowing down of fusion products. Nevertheless, in present fusion experiments on tokamaks, the main energetic particles come from auxiliary systems. For discharges heated with neutral beam injection (NBI) and ion cyclotron resonance heating (ICRH), fast ions are first generated by NBI and then further accelerated by ICRH. Self-consistent modeling of the interactions between ICRH and fast ions from NBI is important for both present-day fusion experiments and for the future ITER and CFETR reactors.

For DD discharges on EAST, 2.45 MeV neutrons are produced in $D + D \rightarrow n(2.45 \text{ MeV}) + {}^3\text{He}(0.82 \text{ MeV})$ reactions. Therefore, neutron emission measurements could be applied to evaluate the

effects of auxiliary heating, providing kinetic information related to burning plasmas such as fast ion velocity distributions. The neutron diagnostic systems in EAST, including a radial neutron camera,¹ a neutron flux monitor,¹ and two compact and one time-of-flight enhanced diagnostic (TOFED) neutron emission spectrometers,²⁻⁶ have been applied to fast ion diagnostics. Significant progress on high-performance plasma discharges with high power auxiliary heating has been achieved at EAST over the last several years.⁷⁻⁹

The NBI-ICRH synergy leads to NBI-generated fast ion acceleration, which can be diagnosed and understood by the neutron emission spectroscopy and numerical simulations. Previously, the NBI-ICRH synergy has been investigated on JET^{10,11} and ASDEX-U.¹² This is the first successful demonstration of NBI-ICRH synergy scenario at EAST. In this work, focusing on the EAST

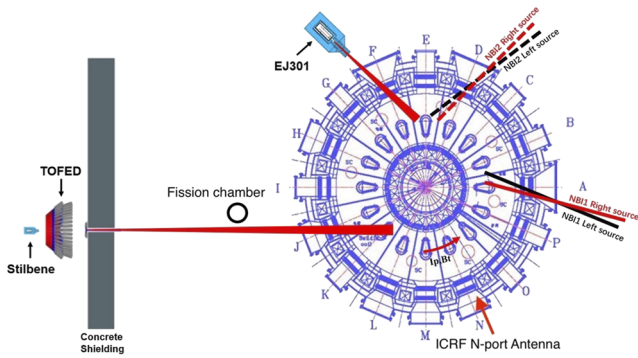


FIG. 1. Schematics of the EAST, including the ^{235}U fission chamber, TOFED, CNS stilbene on the J-port, CNS EJ301 on the F-port, NBI on the A- and D-ports, and ICRH on the N-port.

NBI-ICRH synergistic heating discharges, we present the calculated neutron yield benchmarked by a ^{235}U fission chamber, the fast ion velocity distributions, and the calculated neutron emission spectrum (NES).

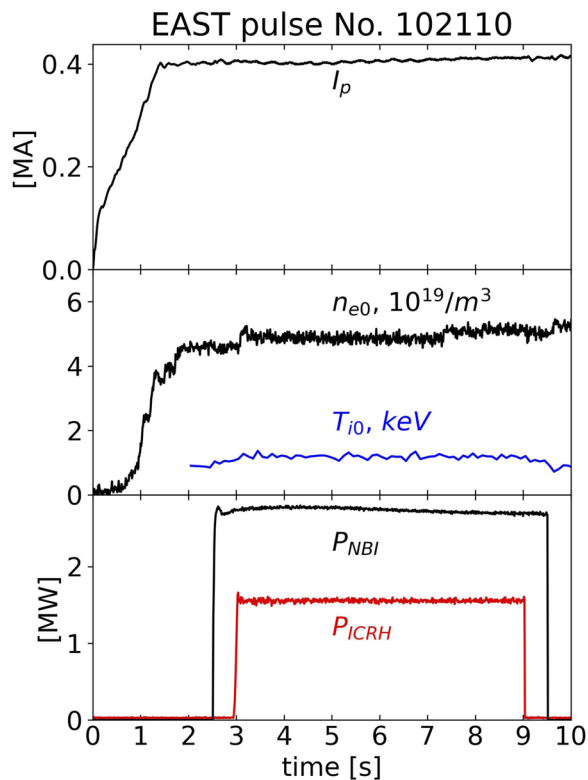


FIG. 2. Time traces of EAST pulse No. 102110. From top to bottom are the time traces of plasma current, I_p , central electron density, n_{e0} , central ion temperature, T_{i0} , NBI, and ICRH heating power, P_{NBI}/P_{ICRH} .

II. NBI-ICRH SYNERGISTIC HEATING ON EAST

EAST is the world's first fully superconducting non-circular cross section tokamak aiming at investigating the technology and physics of high-performance and long pulse operations on next-step advanced fusion devices.¹³ Figure 1 presents the top view of EAST installed with NBI and ICRH auxiliary heating systems, a standard ^{235}U fission chamber, two compact neutron spectrometers (CNSs) of stilbene and EJ301, and a TOFED neutron spectrometer. The EAST tokamak is built with a major radius $R = 1.85$ m, minor radius $a = 0.45$ m, toroidal field $B_t \leq 3.5$ T, plasma current $I_p \leq 1$ MA, and expected plasma pulse length up to 1000 s. The EAST NBI system with a total beam power of up to 8 MW is composed of two neutral beam (NB) injectors, each of which includes two independent beam channels. In the latter half of 2020, some extensive upgrades were made on EAST. One of the significant upgrades was to relocate one NB injector from the F-port to the D-port.¹⁴ As a result, all beamline directions are clockwise-injection. An EAST ICRH antenna is installed on the N-port at a working frequency of 37 MHz for the hydrogen minority ICRH regime with a total power of around 2 MW. The concentration of hydrogen in deuterium plasma is usually about 4%.

EAST pulse No. 102110, Fig. 2, was carried out in an HD mixture with $H/D \approx 4\%$, plasma current of $I_p \approx 0.4$ MA, magnetic field of $B_0 \approx 2.28$ T, central electron density of $n_{e0} \approx 5.2 \times 10^{19} \text{ m}^{-3}$, and central ion temperature of $T_{i0} \approx 1.2$ keV. Around 2.75 MW NBI-D and 1.42 MW ICRH are applied to the deuterium plasma. The full energy of NB is 55 keV. The usual half and third energy components of NB account for 17.13% and 7.78%, respectively.¹⁵ Pulse No. 102111 was carried out without ICRH, and the other conditions were nearly the same as pulse No. 102110.

III. FAST NBI-D ION ACCELERATION BY ICRH

The NBI-ICRH synergistic heating on EAST has been recently simulated by the TRANSP code,¹⁶ including the full wave solver TORIC code¹⁷ and the Monte Carlo NUBEAM code.¹⁸ The radio frequency (RF)-wave field is calculated by TORIC and passed to NUBEAM inside TRANSP. We used 16 processors on the ShenMa High Performance Computing Cluster in the Institute of Plasma Physics, Chinese Academy of Sciences. For TRANSP analysis time equivalent to 1.0 s, it takes 670 h of central processing unit (CPU) time for an NBI-ICRH phase and 463 h of CPU time for an NBI-only phase. Figure 3 shows the contour plots of the amplitude of the RF electric field [(a) left-handed component $|E_+|$ and (b) right-handed component $|E_-|$]; 2D profiles of power density to (c) NBI-generated ions and (d) bulk thermal ions for EAST discharge No. 102110 at 5.80 s). As can be seen in Fig. 3(a), the long wavelength fast wave (FW) launched from the low-field side midplane is converted near the Ion-Ion Hybrid (IIH) layer into the short wavelength ion Bernstein wave (IBW, emanating leftward, toward the high field side), heating electrons via electron Landau damping (ELD).² In addition, the left-handed RF electric field amplitude $|E_+|$ is maximized near the IIH layer, which in hot plasma becomes a Mode Conversion (MC) layer. In pulse No. 102110, NBI fast ions and bulk thermal ions are heated at the second harmonic resonance by RF waves, and the 2D profiles of absorbed RF power density are shown in Figs. 3(c) and 3(d), respectively.

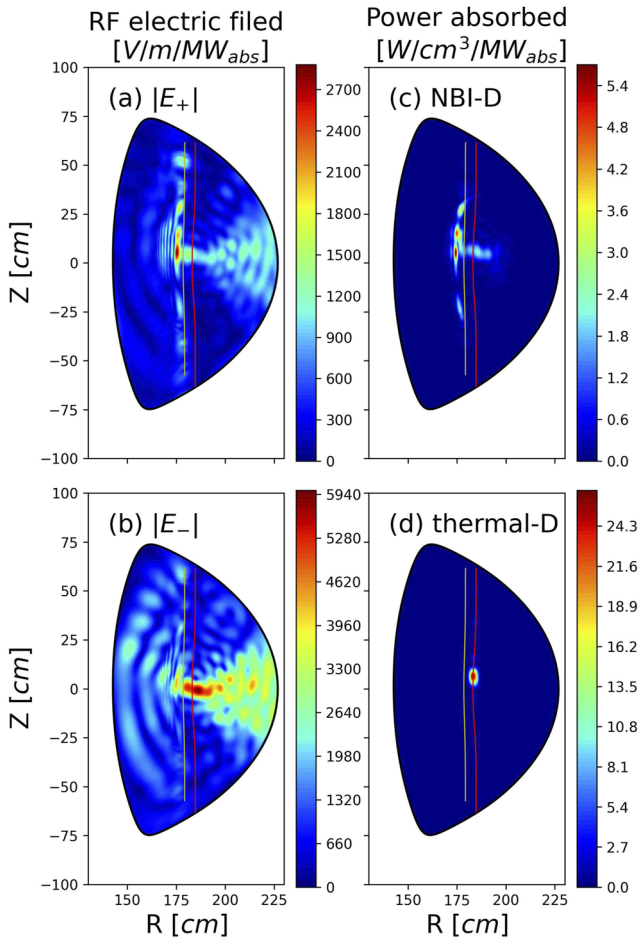


FIG. 3. Contour plots of the amplitude of the RF electric field: (a) left-handed component $|E_+|$ and (b) right-handed component $|E_-|$; 2D profiles of power density to (c) NBI-generated ions and (d) bulk thermal ions for EAST discharge No. 102110 at 5.80 s. The red vertical line indicates the second harmonic resonance layer, and the yellow vertical line indicates the Ion-Ion Hybrid (IIH) layer.

The NUBEAM module calculates the fast NBI-D ion slowing down distribution function,³ and the left-handed component of the RF electric field, E_+ rotating in the ion Larmor motion direction, accelerates fast NBI-D ions, satisfying the wave-particle resonance condition.² Moreover, with the RF-kick operator¹⁹ implemented in TRANSP, we can calculate the effects of ICRH on the NBI-generated fast ions. This is a quasi-linear diffusion process and the main term of the diffusion operator,^{19,20}

$$D_{RF} \propto |E_+|^2 J_{n-1}^2(k_{\perp} \rho_{ci}), \quad (1)$$

where J_m , n , k_{\perp} , and ρ_{ci} are the m th order Bessel function, harmonic number, perpendicular angular wave number, and ion cyclotron radius, respectively. Hence, harmonic heating is a finite Larmor radius (FLR) effect if the ion Larmor radius is comparable to the RF wavelength. In addition, the fast ion velocity diffusion degree depends on the amplitude of the left-handed RF electric field. As a

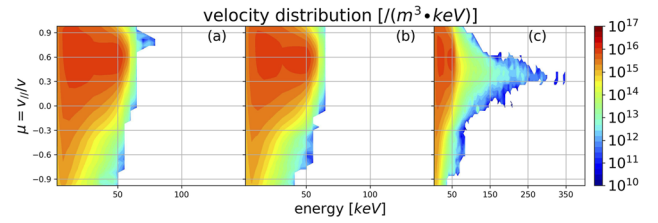


FIG. 4. Volume averaged energy/pitch fast ion velocity distributions of D ions at 5.80 s from TRANSP simulations of (a) shot No. 102111 (NBI-phase) and shot No. 102110 (NBI-ICRH phase) simulation (b) without and (c) with an RF-kick.

result, the maximum power absorbed by NBI-D is near the IIH layer, which is similar to $|E_+|$, while the maximum of power absorbed by thermal-D is located at the second harmonic resonance layer. The calculation model takes no account of the RF interactions with edge plasma and the plasma wall.¹⁷ Meanwhile, the right-handed wave field E_- and the parallel wave field E_{\parallel} are neglected in Eq. (1) and in the implementation.²⁰

Despite these limitations, TRANSP has been successfully applied to simulate NBI-ICRH synergistic heating on JET¹¹ and ASDEX-U.¹² Through this approach, focusing on the EAST discharge Nos. 102110 and 102111, the volume averaged fast ion distribution functions at 5.80 s modeled by TRANSP are shown in Fig. 4. Figure 4(a) shows the fast ion distribution function of shot No. 102111 (only NBI phase) and the case of shot No. 102110 (NBI-ICRH phase) (b) without the RF-kick operator and (c) with the RF-kick operator. The fast ion distribution functions for cases (a) and (b) are nearly the same, while those for (b) and (c) are quite different, indicating the RF-kick operator is crucial to include in modeling the effect of RF waves on accelerating fast ions. In pulse No. 102110, fast NBI-D ions are accelerated far exceeding the NBI energy of 55 keV, and the maximal energy reaches 350 keV. Such energetic tails will strongly intensify the fusion reactions in burning plasmas.

IV. OBSERVATIONAL EFFECTS OF FAST ION ENERGETIC TAILS

A. Increase in the neutron emission rates

The neutral beam deuterons accelerated by second harmonic RF heating in EAST leads to a substantial increase in fusion neutron production, which can be detected by an *in situ* calibrated ²³⁵U fission chamber. Figure 5(a) presents the time traces of the neutron yield calculated by TRANSP and compared those with the ²³⁵U fission chamber experimental data with error bars. As shown in Fig. 5(a), the neutron yield of pulse No. 102110 is approximately twice that of pulse No. 102111. This is due to the supra-thermal ions from ICRH and the positive energy-dependence of the fusion reaction cross-sections.

B. Broadening of the neutron emission spectra

On EAST tokamak, two scintillator-based CNSs, EJ301 and stilbene, are available with parallel views through the plasma equatorial plane, allowing us to infer the fast ion distribution functions, in

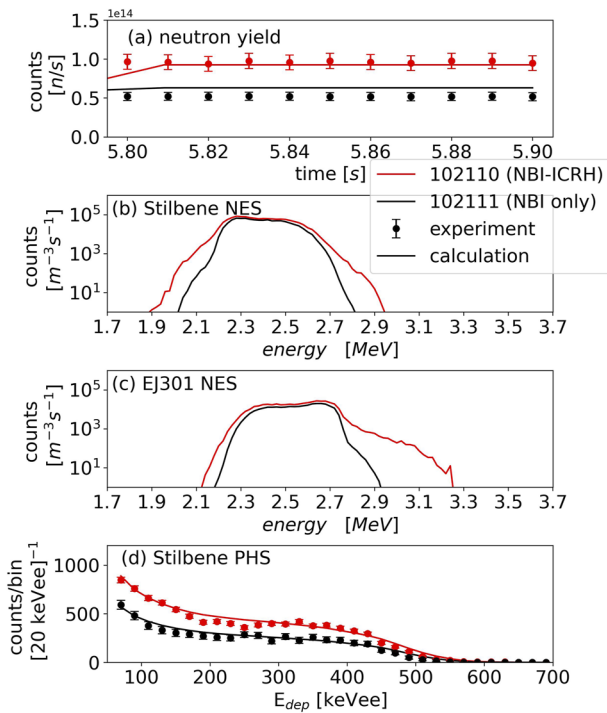


FIG. 5. (a) Time traces of the neutron yield calculated by TRANSP in lines and compared with the ^{235}U fission chamber experiments in dots with error bars; the neutron energy spectrum calculated by TRANSP and GENESIS in the line-of-sight of the compact neutron spectrometer (b) stilbene and (c) EJ301; (d) calculated and measured pulse height spectra of discharge Nos. 102110 (NBI-ICRH phase) and 102111 (NBI-only phase).

particular the supra-thermal components. The NES could be numerically computed by the Monte Carlo code GENESIS,²¹ which is capable of calculating an NES from a given non-Maxwellian fast ion velocity distribution function and given bulk thermal ion temperature and density profiles in a given line-of-sight. In the TRANSP simulation, the ion density n_i was calculated by electron density n_e and line-averaged effective charge Z_{eff} . Electron temperature and density measured data were obtained from the collective Thomson scattering diagnostic²² at the EAST. The ion temperature is monitored by using the tangential x-ray imaging crystal spectrometer (TXCS).²³ Using these experimental parameters and the simulated fast ion velocity distribution functions by the TRANSP code, the calculated neutron spectra in the line-of-sight of the stilbene and EJ301 spectrometers are shown in Figs. 5(b) and 5(c), respectively. The neutron spectra for the NBI-ICRH phase are obviously wider than those of the NBI-only phase, verifying the energetic tails in fast ion distributions due to RF heating. Figure 5(d) presents the pulse height spectra (PHSs) measured by the stilbene neutron spectrometer for discharge Nos. 102110 and 102111, which are calculated after modeling the neutron scattering with the MCNP code²⁴ and folding the NESs with the CNS response matrix. The agreement between the calculated results and experimental data validates the NBI-generated fast ion acceleration on EAST NBI-ICRH synergistic heating scenarios.

V. CONCLUSIONS

We focused on the observational enhancements of neutron measurements in the NBI-ICRH synergy scenario and chose two discharges to analyze in this paper, proving that this scenario could be successfully executed on EAST. The RF-kick operator implemented in TRANSP realizes a quantitative calculation of the fast ion velocity diffusion process in the kinetic level due to RF heating. The acceptable agreement between calculations and experiments validates that the NBI-generated fast ion satisfying the wave-particle resonance condition could be accelerated by ICRH to a much higher energy than the injection beam energy, which can be detected by neutron flux monitors and CNSs. The CNS EJ301 and TOFED experimental results are still under processing and will be compared with simulations in the near future.

ACKNOWLEDGMENTS

This work was supported by the National MCF Energy R&D Program (Grant Nos. 2019YFE03040000, 2013GB106004, and 2012GB101003), the National Key Research and Development Program of China (Grant Nos. 2016YY0200805 and 2017YFF0206205), the State Key Program of National Natural Science of China (Grant No. 11790324), and the User with Excellence Program of Hefei Science Center CAS (Grant No. 2020HSC-UE012). The authors are very grateful to the members of the EAST operation team for their help during the experimental campaigns.

AUTHOR DECLARATIONS

Conflict of Interest

The authors have no conflicts to disclose.

Author Contributions

D. K. Yang: Conceptualization (equal); Data curation (equal); Formal analysis (equal); Software (equal); Validation (equal); Visualization (equal); Writing – original draft (equal); Writing – review & editing (equal). **L. Y. Liao:** Data curation (equal). **Y. H. Li:** Data curation (equal). **G. Q. Zhong:** Data curation (equal). **X. J. Zhang:** Formal analysis (equal). **W. Zhang:** Formal analysis (equal). **B. L. Hao:** Software (equal). **L. Q. Hu:** Investigation (equal). **B. N. Wan:** Investigation (equal). **Z. M. Hu:** Investigation (equal). **Y. M. Zhang:** Investigation (equal). **G. Gorini:** Investigation (equal). **M. Nocente:** Investigation (equal). **M. Tardocchi:** Investigation (equal). **X. Q. Li:** Investigation (equal). **C. J. Xiao:** Investigation (equal). **T. S. Fan:** Funding acquisition (lead).

DATA AVAILABILITY

The data that support the findings of this study are available from the corresponding authors upon reasonable request.

REFERENCES

- G. Q. Zhong, L. Q. Hu, N. Pu, R. J. Zhou, M. Xiao, H. R. Cao, Y. B. Zhu, K. Li, T. S. Fan, X. Y. Peng *et al.*, *Rev. Sci. Instrum.* **87**, 11D820 (2016).
- L. J. Ge, Z. M. Hu, Y. M. Zhang, J. Q. Sun, X. Yuan, X. Y. Peng, Z. J. Chen, T. F. Du, G. Gorini, M. Nocente *et al.*, *Plasma Phys. Controlled Fusion* **60**, 095004 (2018).

- ³X. Yuan, X. Zhang, X. Xie, G. Gorini, Z. Chen, X. Peng, J. Chen, G. Zhang, T. Fan, G. Zhong *et al.*, *J. Instrum.* **8**, P07016 (2013).
- ⁴X. Zhang, X. Yuan, X. F. Xie, Z. J. Chen, X. Y. Peng, J. X. Chen, G. H. Zhang, X. Q. Li, T. S. Fan, G. Q. Zhong *et al.*, *Rev. Sci. Instrum.* **84**, 033506 (2013).
- ⁵X. Zhang, Z. J. Chen, X. Y. Peng, Z. M. Hu, T. F. Du, Z. Q. Cui, X. F. Xie, X. Yuan, T. S. Fan, J. Kallne *et al.*, *Nucl. Fusion* **54**, 104008 (2014).
- ⁶L. J. Ge, Z. M. Hu, Y. M. Zhang, J. Q. Sun, X. Yuan, X. Y. Peng, Z. J. Chen, T. F. Du, M. Nocente, G. Gorini *et al.*, *Rev. Sci. Instrum.* **89**, 10I143 (2018).
- ⁷B. N. Wan, J. G. Li, H. Y. Guo, Y. F. Liang, G. S. Xu, and X. Z. Gong for the EAST Team, International Collaborators, *Nucl. Fusion* **53**, 104006 (2013).
- ⁸B. N. Wan, EAST Team and Collaborators, *Plasma Phys. Controlled Fusion* **58**, 014029 (2016).
- ⁹X. Gao, Y. Yang, T. Zhang, H. Q. Liu, G. Q. Li, T. F. Ming, Z. X. Liu, Y. M. Wang, L. Zeng, X. Han *et al.*, *Nucl. Fusion* **57**, 056021 (2017).
- ¹⁰C. Hellesen, M. G. Johnson, E. A. Sundén, S. Conroy, G. Ericsson, E. Ronchi, H. Sjöstrand, M. Weiszflog, G. Gorini, M. Tardocchi *et al.*, *Nucl. Fusion* **50**, 022001 (2010).
- ¹¹K. K. Kirov, Y. Kazakov, M. Nocente, J. Ongena, Y. Baranov, F. Casson, J. Eriksson, L. Giacomelli, C. Hellesen, V. Kiptily *et al.*, *AIP Conf. Proc.* **2254**, 030011 (2020).
- ¹²G. Tardini, R. Bilato, R. Fischer, M. Weiland, and ASDEX Upgrade Team, *Nucl. Fusion* **59**, 046002 (2019).
- ¹³J. Li, H. Y. Guo, B. N. Wan, X. Z. Gong, Y. F. Liang, G. S. Xu, K. F. Gan, J. S. Hu, H. Q. Wang, L. Wang *et al.*, *Nat. Phys.* **9**, 817–821 (2013).
- ¹⁴J. Wang, J. L. Chen, B. Wu, Y. Q. Chen, Z. Yang, C. D. Hu, Y. L. Xie, Y. H. Xie, and X. X. Zhang, *Phys. Scr.* **96**, 075604 (2021).
- ¹⁵C. D. Hu, Y. H. Xie, Y. L. Xie, S. Liu, Y. J. Xu, L. Z. Liang, C. C. Jiang, P. Sheng, Y. M. Gu, J. Li *et al.*, *Plasma Sci. Technol.* **17**, 817 (2015).
- ¹⁶J. Breslau, M. Gorelenkova, F. Poli, J. Sachdev, A. Pankin, G. Perumpilly, X. Yuan, and L. Glant, TRANSP: Computer Software, USDOE Office of Science (SC), Fusion Energy Sciences (FES) (SC-24), 27 June 2018.
- ¹⁷M. Brambilla, *Plasma Phys. Controlled Fusion* **41**, 1 (1999).
- ¹⁸A. Pankin, D. McCune, R. Andre, G. Bateman, and A. Kritiz, *Comput. Phys. Commun.* **159**, 157–184 (2004).
- ¹⁹T. H. Stix, *Nucl. Fusion* **15**, 737 (1975).
- ²⁰N. Bertelli, M. Gorelenkova, M. Podesta, E. Valeo, D. Green, and E. Fredrickson, *EPJ Web Conf.* **157**, 03004 (2017).
- ²¹M. Nocente, *Neutron and Gamma-Ray Emission Spectroscopy as Fast Ion Diagnostics in Fusion Plasmas* (Università degli Studi di Milano-Bicocca, 2012).
- ²²S. Xiao, Q. Zang, A. Hu, X. Han, J. Hu, X. Zhang, and Y. Gu, *Fusion Eng. Des.* **158**, 111675 (2020).
- ²³F. Wang, J. Chen, R. Hu, B. Lyu, G. Colledani, J. Fu, Y. Li, M. Bitter, K. Hill, S. Lee *et al.*, *Rev. Sci. Instrum.* **87**, 11E342 (2016).
- ²⁴X-5 Monte Carlo Team, MCNP: A General Monte Carlo N-Particle Transport Code, Version 5 I 2-71-2-80, Los Alamos National Laboratory, 2005.